Phytochemistry 197 (2022) 113122

Contents lists available at ScienceDirect

Phytochemistry

journal homepage: www.elsevier.com/locate/phytochem

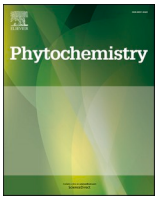

Density functional theory study on the coupling and reactions of diferuloylputrescine as a lignin monomer

Thomas Elder [a,*], José C. del Río [b], John Ralph [c,d], Jorge Rencoret [b], Hoon Kim [c]

[a] USDA-Forest Service, Southern Research Station, 521 Devall Drive, Auburn, AL, 36849, USA
[b] Instituto de Recursos Naturales y Agrobiología de Sevilla (IRNAS), CSIC, Av. Reina Mercedes, 10, 41012, Seville, Spain
[c] Department of Energy Great Lakes Bioenergy Research Center, Wisconsin Energy Institute, University of Wisconsin, 1552 University Ave, Madison, WI, 53726, USA
[d] Department of Biochemistry, University of Wisconsin, 433 Babcock Drive, Madison, WI, 53706, USA

ARTICLE INFO

Keywords:
Diferuloylputrescine
Homo-couple
Cross-couple
Density functional theory
Coniferyl alcohol
Lignin
Lignification
Feruloyl amide
Radical coupling

ABSTRACT

Diferuloylputrescine has been found in a variety of plant species, and recent work has provided evidence of its covalent bonding into lignin. Results from nuclear magnetic resonance spectroscopy revealed the presence of bonding patterns consistent with homo-coupling of diferuloylputrescine and the possibility of cross-coupling with lignin. In the present work, density functional theory calculations have been applied to assess the energetics associated with radical coupling, rearomatization, and dehydrogenation for possible homo-coupled dimers of diferuloylputrescine and cross-coupled dimers of diferuloylputrescine and coniferyl alcohol. The values obtained for these reaction energetics are consistent with those reported for monolignols and other novel lignin monomers. As such, this study shows that there would be no thermodynamic impediment to the incorporation of diferuloylputrescine into the lignin polymer and its addition to the growing list of non-canonical lignin monomers.

1. Introduction

The plasticity of lignification towards the incorporation of monomers from beyond the canonical hydroxycinnamyl alcohols (the monolignols coniferyl, sinapyl, and *p*-coumaryl alcohol) has been repeatedly demonstrated and recently reviewed (del Río et al., 2021, 2020; Ralph et al., 2021). At last report there were 35 monomers that may occur naturally or are produced due to genetic modifications (either natural or induced) that have been found in natural lignins (Ralph et al., 2019; Vanholme et al., 2019). Included are monolignol ester conjugates (with ferulates, acetates, *p*-hydroxybenzoates, *p*-coumarates, vanillates, or benzoates) (del Río et al., 2008, 2007; Karlen et al., 2017, 2016; Kim et al., 2020; Lu et al., 2015), the catechyl alcohols (caffeyl and 5-hydroxyconiferyl alcohol) (Chen et al., 2012; Ralph et al., 2001), and dihydroconiferyl alcohol and hydroxycinnamaldehydes (Ralph et al., 1997), all of which are derived from the general phenylpropanoid pathway. Subsequently, lignin monomers arising from other metabolic pathways (i.e., a hybrid of the phenylpropanoid and acetate/malonate polyketide pathway or the amino acid pathway) have been identified (del Río et al., 2021, 2020). These include the hydroxystilbenes and their glucosylated derivatives (del Río et al., 2017; Rencoret et al., 2019, 2018), the flavone tricin (del Río et al., 2012; Lan et al., 2016b, 2016a, 2015), the nitrogen-containing feruloyltyramine, and the subject of the current paper diferuloylputrescine (del Río et al., 2018; Kudanga et al., 2009; Negrel et al., 1996; Ralph et al., 1998).

Diferuloylputrescine (Fig. 1) has been found in extracts from corn (*Zea mays*) and corn oil (Moreau et al., 2001; Moreau and Hicks, 2005), as well as in bamboo (*Phyllostachys heterocycla*) (Yoshimura et al., 2017). Beyond botanical interest, diferuloylputrescine has been found to be quite active biologically. In a study of antiprotozoal activity, diferuloylputrescine was found in the chloroform extracts of *Haplophyllum tuberculatum* roots; among the compounds isolated it was found to be the most effective against *Trypanosoma brucei rhodesiense,* which causes sleeping sickness (Mahmoud et al., 2020). Other work on extracts from corn has found that diferuloylputrescine has high antioxidant activity (Bauer et al., 2012, 2013), anti-inflammatory and anti-melanogenic properties (Kim et al., 2010, 2012), inhibits aflatoxin production (Mellon and Moreau, 2004), and is inhibitory to α-glucosidase, a property that can have applications in diabetes treatments (Niwa et al., 2003).

In a study on the milled wood lignin (MWL) and dioxane lignin (DL) preparations isolated from corn grain fibers, the presence of diferuloylputrescine was detected by the application of 2D HSQC NMR (del

* Corresponding author.
E-mail address: thomas.elder@usda.gov (T. Elder).

https://doi.org/10.1016/j.phytochem.2022.113122
Received 14 September 2021; Received in revised form 25 January 2022; Accepted 29 January 2022
Available online 5 February 2022
0031-9422/Published by Elsevier Ltd.

Río et al., 2018). The detailed assignments demonstrating the occurrence of diferuloylputrescine were determined by 2D HSQC-TOCSY and HMBC NMR experiments. The latter are consistent with literature spectra and have been confirmed with a synthetically prepared authentic standard. As discussed previously, free diferuloylputrescine can be extracted with organic solvents, and the corn fiber in the referenced paper had been subjected to exhaustive extraction with acetone, methanol and water. This demonstrated that the diferuloylputrescine detected in the isolated lignins was covalently bonded to the cell wall and was not a residual free compound. The NMR experiments also provided evidence of 8-5' phenylcoumaran linkages involving diferuloylputrescine, showing that homo-coupled dimers or higher oligomers may occur along with the possibility of cross-coupling to ferulates or lignin. Feruloyl amides, which include diferuloylputrescine, are substrates for peroxidase enzymes *in vitro* such that the resultant phenoxy radicals (Fig. 1) could couple through the 5-, 8- and 4-O- positions by radical addition to another diferuloylputrescine, ferulates, or monolignols, followed by rearomatization, becoming integrated into the cell wall. Based on these possible reactive sites, diferuloylputrescine could act as a branch point within the lignin polymer, resulting in a cross-linked network and, as two phenolic groups are present, lignification could occur at both phenolic ends.

To date, the 8-5' linkage has been unambiguously identified, whereas other potential coupling products, such as 8-O-4' or 5-5', have only been tentatively identified by NMR and await confirmation. The objective of the current work is therefore to determine if the reactions required for the formation of the homo-coupled and cross-coupled products are energetically feasible. This question will be addressed by the application of contemporary methods in computational chemistry to the proposed reactants and products associated with homo-coupling of diferuloylputrescine and its cross-coupling with monolignols. In addition, given the documented medicinal value of diferuloylputrescine, its release from plant tissues may provide a new source of this compound. As such, the bond dissociation energies of the homo-coupled and cross-coupled dimers will be determined to assess the potential for liberation of diferuloylputrescine. Furthermore, as the dimers have at least two phenolic groups, and could potentially react through all of them, the energy associated with dehydrogenation at these points will be determined. The computational work flow described in the current submission involving a force-field-based conformational search followed by refinement with one or more electronic structure methods is consistent with previously published papers (by ourselves and others) concerned with the conformation and reactivity of isolated lignin structures. This process has undergone extensive peer review and has also been successfully applied to the non-canonical lignin monomers piceatannol, tricin, and the catechyl alcohols. (Berstis et al., 2016, 2020; Elder et al., 2016, 2019, 2020; Kim et al., 2011; Sangha et al., 2012, 2014).

2. Results and discussion

2.1. Dehydrogenation of diferuloylputrescine

The energy of diferuloylputrescine dehydrogenation (Fig. 1) at 76.6 kcal mol^{-1} is comparable to that of the canonical monolignols (coniferyl alcohol, 77.1 kcal mol^{-1}; sinapyl alcohol, 72.8 kcal mol^{-1}; *p*-coumaryl alcohol, 76.4 kcal mol^{-1}), as well as other non-conventional lignin monomers such as piceatannol (76.4 kcal mol^{-1}) (Elder et al., 2019) and the hydroxystilbene glucosides (75.8–76.8 kcal mol^{-1}) (Elder et al., 2021). The optimized structures of diferuloylputrescine and its dehydrogenation product are shown in Fig. 2. The most striking observation of the monomer and radical structures is the markedly folded conformations in which the aromatic rings are at distances of 3.60 and 3.58 Å, respectively. The rings are also essentially parallel with an inter-plane angle of 6.72° for the diferuloylputrescine and 4.87° for the radical. These conformations and inter-ring distances are consistent with the sandwich geometry of aromatic dimers in which π-stacking is proposed to occur (Sinnokrot and Sherrill, 2004). Fig. 2 also shows that the locations of unpaired spin density of the diferuloylputrescine radical are consistent with the predicted resonance structures in Fig. 1 and with those of the monolignols.

It should also be noted that these observed geometries are the result of gas phase calculations. The conformations were further investigated with implicit solvation with water, resulting in the structures shown in Fig. 2. It can be seen that the folded geometry is retained upon solvation for both the closed-shell and radical forms of diferuloylputrescine.

2.2. Radical coupling and rearomatization

2.2.1. Homo-coupled diferuloylputrescine

The free energies of radical coupling and rearomatization for the several homo-coupled dimers are as shown in Fig. 3. Among the intermediates resulting from the radical coupling step, the 8-O-4' quinone methide is the most stable and therefore its formation is the most exergonic. The radical coupling step in this case generates a single new chiral center. Among the 8-5' quinone methide and the 5-5' dicyclohexadienone intermediates, both of which involve carbon-carbon bond formation, the latter intermediates that involve two aromatic centers, are less stable by ~6–12 kcal mol^{-1}. These lowered stabilities can be attributed to larger reductions in aromaticity upon coupling. Radical coupling through the 8-5' and 5-5' positions generates two chiral centers each, for which there is some degree of stereochemical preference at 4.2 and 2.2 kcal mol^{-1}, respectively.

The rearomatization reactions follow a predictable pattern with the 5-5' dimer, which involves carbon-carbon bond formation, as the most exergonic, and the carbon-oxygen bonded 8-O-4', as the least. The 8-5' product in which both carbon-carbon and carbon-oxygen bonds are formed along with ring closure varies with stereochemistry, wherein the

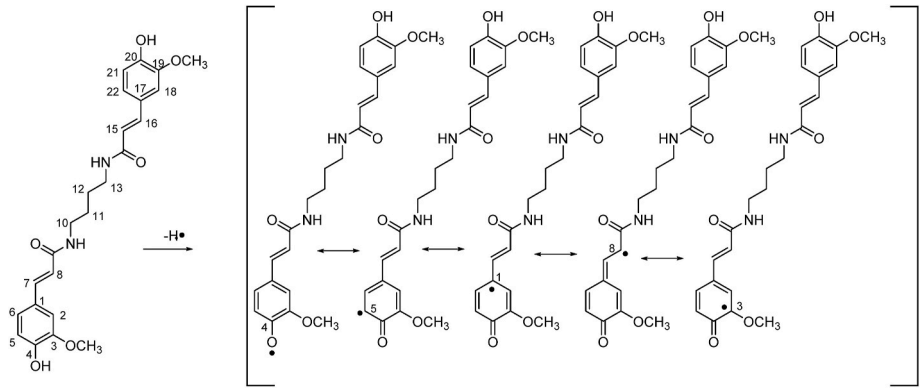

Fig. 1. Diferuloylputrescine and resonance structures from dehydrogenation.

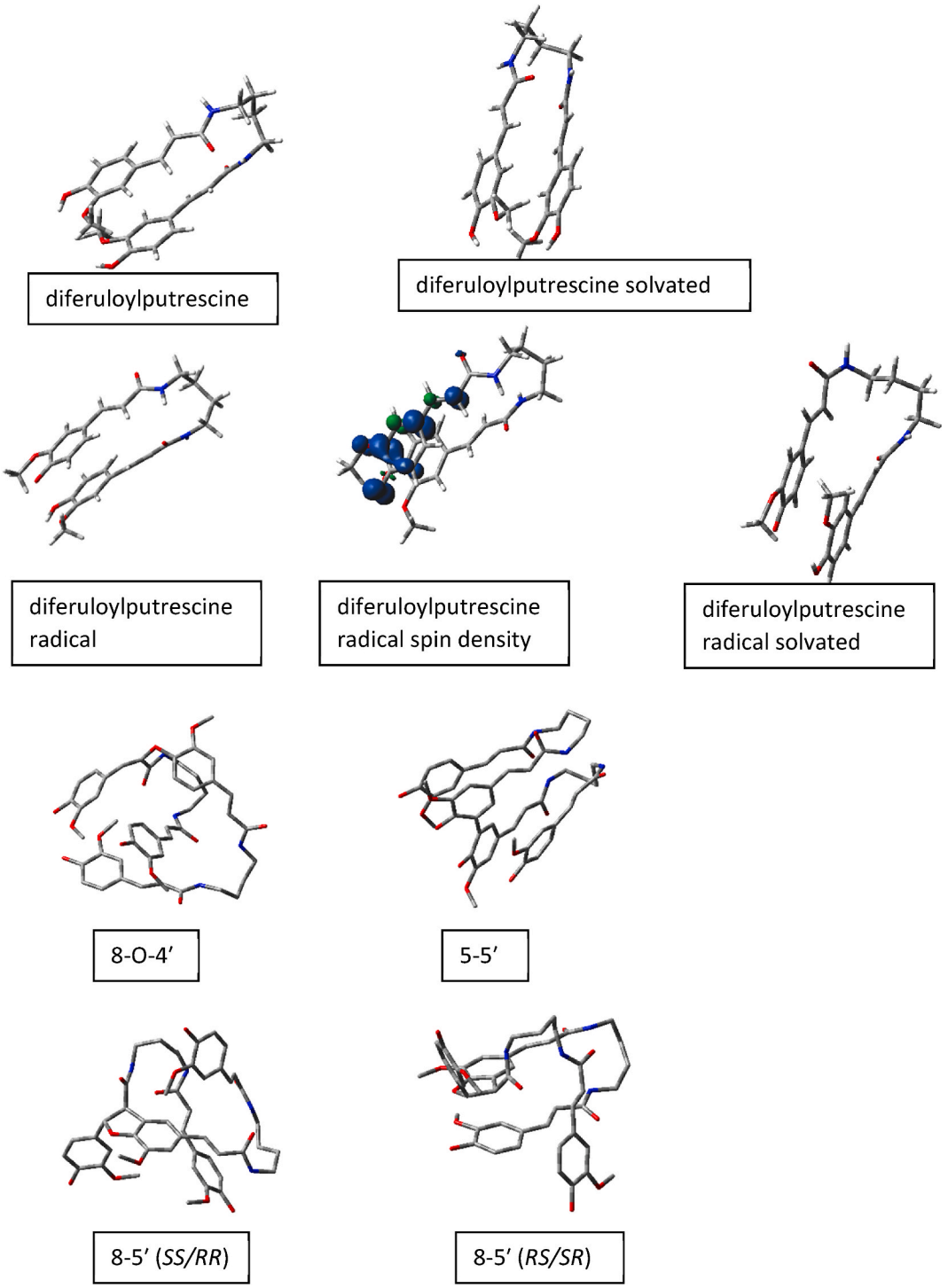

Fig. 2. Optimized geometries for diferuloylputrescine, the diferuloylputrescine radical (with spin densities) and homo-coupled diferuloylputrescine dimers.

RS/SR stereoisomer, is the most stable of the dimeric products, although the difference with 5-5' (0.6 kcal mol^{-1}) is within the accuracy of the density functional theory method used in this work (0.4–1.3 kcal mol^{-1}) (Zhao and Truhlar, 2008), such that they cannot be differentiated based on energy. Furthermore, the low energy *RS/SR* stereoisomer of the 8-5' dimer corresponds to the *cis* conformation, rather than the *trans* configuration routinely found in lignin structures (Li et al., 1997; Ralph et al., 2009).

The optimized geometries of the dimers (Fig. 2) are predictably more complex than the monomer, but also exhibit folded conformations. The 8-O-4' and 8-5'-*SS/RR* are twisted and irregular, whereas the aromatic rings of the 5-5' and 8-5'-*SR/RS* dimers are in close proximity and fairly parallel. Within the 5-5' dimer, the torsional angle between rings A and B is 35.21°, the inter-ring distances for rings B-D and A-C are 3.50 and 3.87 Å, with plane angles of 6.62 and 15.97°, respectively. The C-D ring combination of the 8-5'-*SR* is separated by 3.50 Å, with a plane angle of 13.48°. Based on these observations and the differences in energies, stacking of the aromatic rings appears to be contributing to the higher stability of the 5-5' and 8-5'-*SR/RS* dimers.

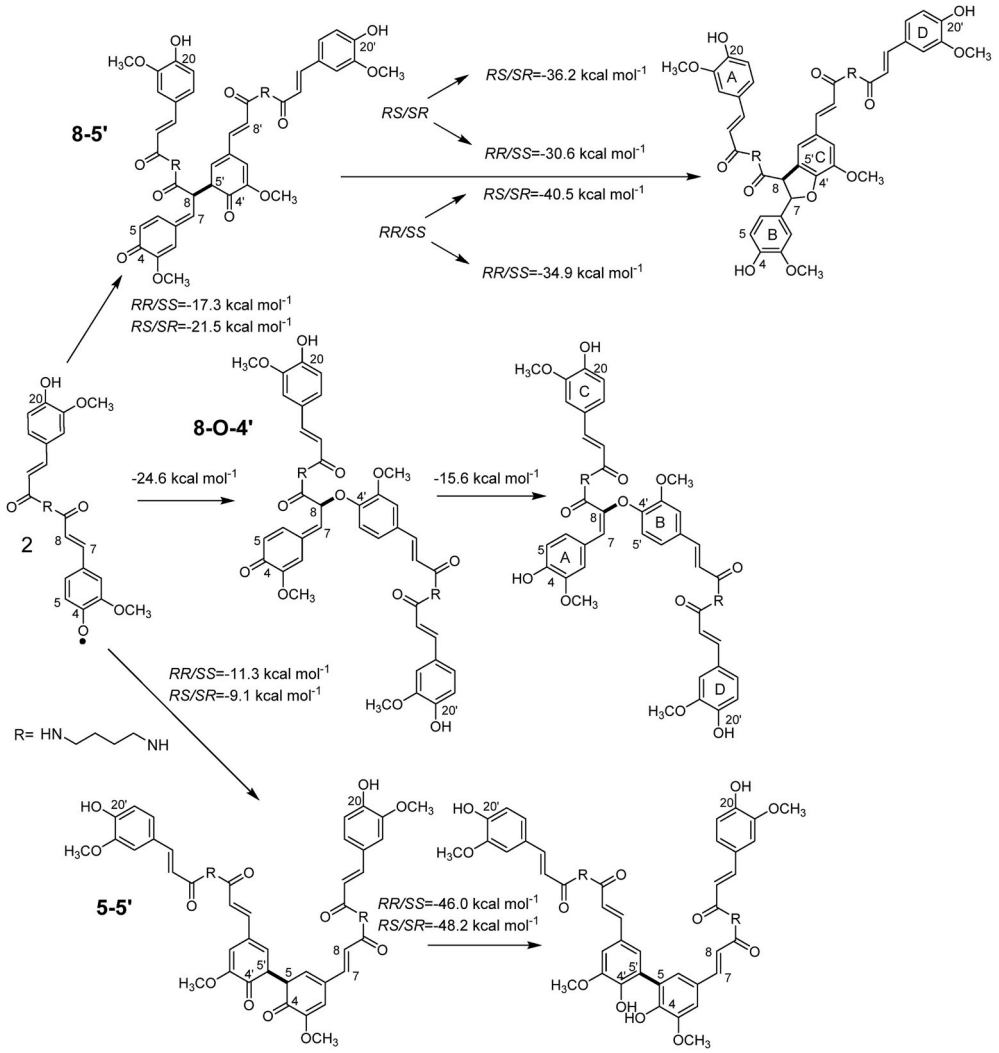

Fig. 3. Gibbs free energies of reaction for radical coupling to form quinone methides and rearomatization for homo-coupled diferuloylputrescine dimers.

2.3. Cross-coupled diferuloylputrescine and coniferyl alcohol

The radical coupling reactions of diferuloylputrescine and coniferyl alcohol are as shown in Fig. 4. The most exergonic of these involve C–O bonds formed through the β'-O-4 and 8-O-4' linkages. Intermediate are the 8-5' and β'-5 linkages that entail bonding between an sp3 carbon and an aromatic carbon. The least exergonic of the cross-coupling reactions is through the 5-5' position, in which both carbons are aromatic. In addition to differences in connectivity, the more exergonic of these retain more aromatic character, resulting in increased stability. In cases for which chiral centers are generated there are small differences (0.6 kcal mol^{-1}, or less) with stereochemistry.

The trend of energetics for the rearomatization reactions, as seen before, is the reverse of that for the radical coupling, with the 5-5' product the most exergonic. Intermediate are the 8-5' and β'-5 products in which a new ether bond is formed along with ring closure. The least exergonic are the acyclic β'-O-4 and 8-O-4' products. Among the 8-5' and β'-5 dimers, which contain phenylcoumaran rings, the low-energy stereoisomers correspond to the *trans* configuration that, as previously noted, is typical in the lignin polymer as well as in analogous neolignans.

The optimized geometries for the cross-coupled dimers are shown in Fig. 5. Due to the smaller size of coniferyl alcohol, these are less folded than the homo-coupled diferuloylputrescine dimers, but there are several instances in which aromatic ring stacking can be observed. Perhaps the most prominent of these occur in the *RR/SS* stereoisomer of the 8-5' dimer. The A-C rings are in a parallel displaced arrangement with a plane angle of 9.76°, but the separation at 4.86 Å is greater than seen in the benzene dimer (Sinnokrot and Sherrill, 2004). The 5-5' dimer also exhibits a parallel displaced conformation, with rings A and C forming a plane angle of 9.53° at a separation of 3.50 Å. Although somewhat organized, the 8-5' *RS/SR* stereoisomer, β'-O-4 RR/*SS* stereoisomer, and β'-5 *RS/SR* have larger plane angles of 10.23, 15.89 and 10.35°, respectively. The *RS/SR* stereoisomer of the β'-O-4 dimer exhibits a T-conformation between the A and B rings, with a plane angle of 88.36° and inter-ring distance of 4.84 Å, which are consistent with the benzene dimer (Sinnokrot and Sherrill, 2004). The 8-O-4' and β'-5 RR/*SS* dimers are irregular. The parallel conformation of the 8-5' *RR/SS* and T-conformation of the β'-O-4 *RS/SR* no doubt contributes to the relative stability over their stereoisomers.

2.4. Energies of hydrogen abstraction and bond dissociation

The energies of hydrogen abstraction and bond cleavage for the homo-coupled dimers of diferuloylputrescine are shown in Fig. 6. The energy of dehydrogenation ranges from 73.9 to 79.5 kcal mol^{-1}, among which the 8-5' dimers are somewhat more endergonic, averaging 78.2 kcal mol^{-1} as opposed to 76.3 kcal mol^{-1} for the 8-O-4' and 5-5' dimers. The bond dissociation energies are much more variable, ranging from 47.1 to 144.1 kcal mol^{-1}. The lowest of these is the triplet formed by cleavage of the 7-O-4' ether bond, whereas the highest, as might be

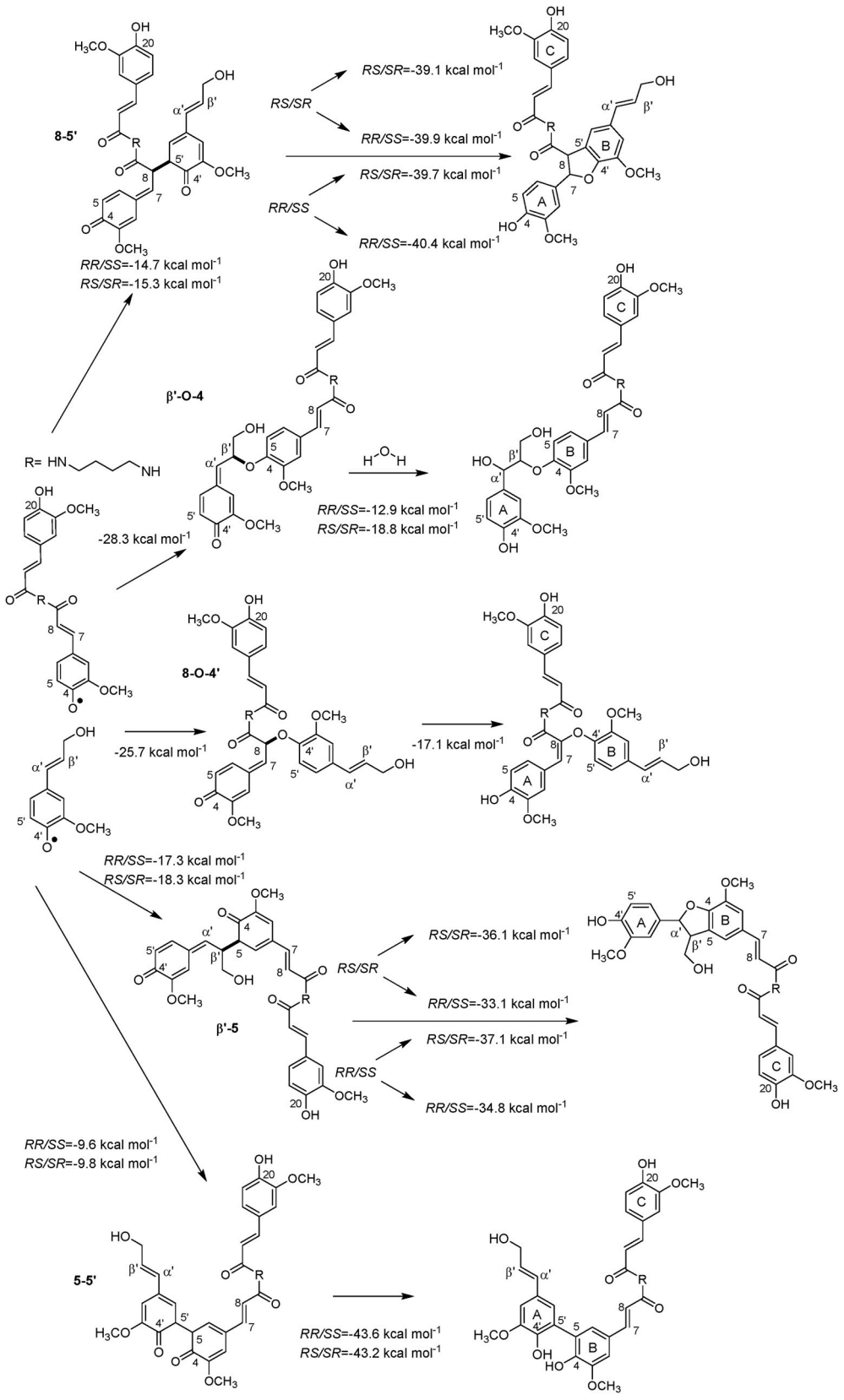

Fig. 4. Gibbs free energies of reaction for radical coupling to form quinone methides and rearomatization for cross-coupled diferuloylputrescine-coniferyl alcohol dimers.

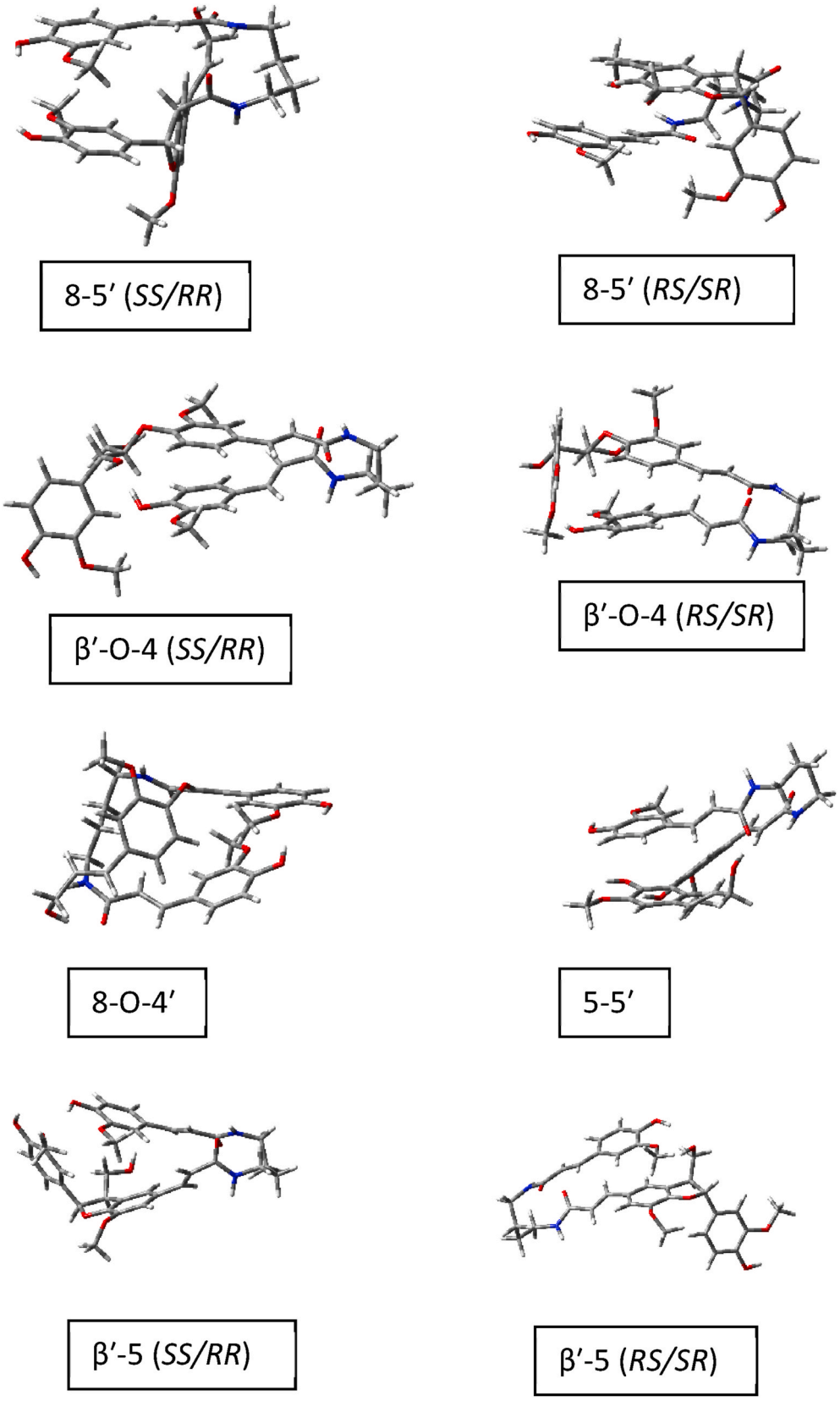

Fig. 5. Optimized geometries for cross-coupled diferuloylputrescine-coniferyl alcohol dimers.

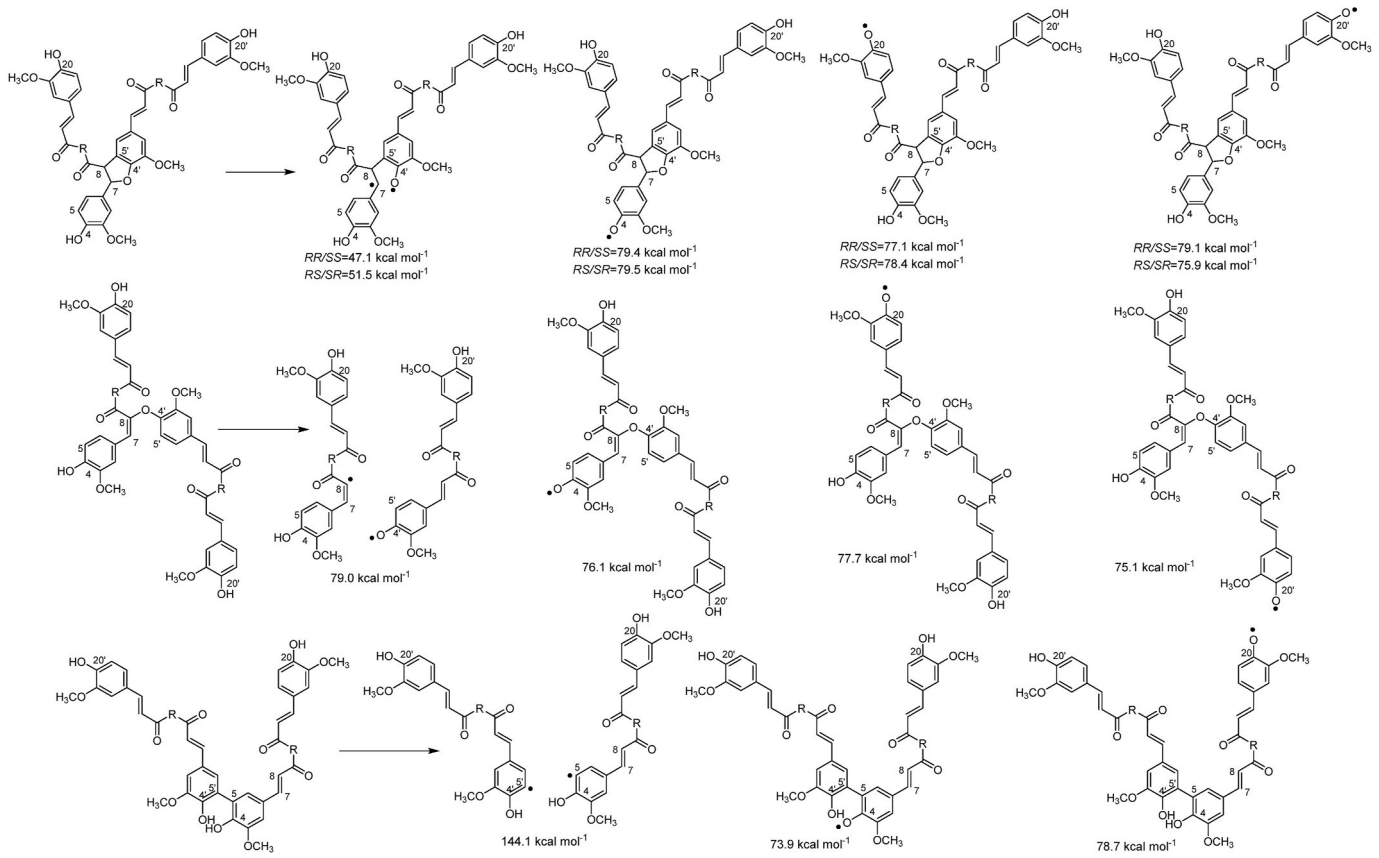

Fig. 6. Gibbs free energy of reaction for dehydrogenation and bond dissociation of homo-coupled diferuloylputrescine dimers.

predicted, is the 5-5' biphenyl bond. Intermediate is the cleavage of the 8-O-4' bond forming two doublets, but at higher energy (79.0 kcal mol^{-1}) due to the sp2 carbon atom at position C-8.

The hydrogen abstraction and bond cleavage reactions for the cross-coupled dimers of diferuloylputrescine and coniferyl alcohol are shown in Fig. 7. The hydrogen abstraction energies range from 73.4 to 80.0 kcal mol^{-1}, among which 5-5' dimers have the lowest average values and the β'-O-4 dimers the highest. The analogous 8-5' and β'-5 cross-coupled dimers are quite similar to each other. The energies of the hydrogen abstraction reactions from the cross-coupled dimers are somewhat lower than both the corresponding homo-coupled dimers in the current work, the cross-coupled dimers of piceatannol and coniferyl alcohol, and the coniferyl alcohol dimer (Elder et al., 2019). The ring-opening reactions of the 8-5' and β'-5 cross-coupled dimers differ with stereochemistry, but do not differ markedly from the 8-5' homo-coupled dimer. Among the bond cleavage reactions generating two doublets, the highest value is, as before, associated with the 5-5' dimer, but is much lower than the corresponding reaction of the homo-coupled dimer. Similarly, the energy of reaction for the cleavage of the 8-O-4' cross-coupled dimer of diferuloylputrescine and coniferyl alcohol at 70.2 kcal mol^{-1} is substantially lower than that of the homo-coupled dimer (79.0 kcal mol^{-1}).

3. Discussion

Comparing the corresponding radical coupling and rearomatization reactions between homo-coupled and cross-coupled dimers of diferuloylputrescine and coniferyl alcohol, the energetics are generally similar. Among the quinone methide formation reactions, the homo-coupled 8-5' products are more exergonic, with larger differences between the stereoisomers. The 8-O-4' reaction energies are quite similar, whereas the 5-5' di-cyclohexadienone are somewhat mixed, with the homo-coupling resulting in larger differences with stereochemistry. Rearomatization of the homo-coupled 8-5' dimers is less exergonic, with differences between the stereoisomers. The rearomatization reaction of the 8-O-4' homo-coupled dimer is less exergonic, whereas the 5-5' is somewhat more exergonic.

In comparison to similar reactions with other non-conventional lignin monomers (Elder et al., 2019), the quinone methides formed by 8-O-4' homo-coupling of two piceatannol units and β-O-4' cross-coupling of piceatannol with coniferyl alcohol have reaction energies of −24.7 and −24.5 kcal mol^{-1}, respectively, such that the latter reaction of diferuloylputrescine and coniferyl alcohol is somewhat more exergonic. In work on hydroxystilbene glucosides (Elder et al., 2021), 8-O-4' coupling of two hydroxystilbene glucosides was considerably less exergonic ranging from −18.4 to −20.5 kcal mol^{-1}. The energies of reaction of hydroxystilbene glucosides cross-coupled with coniferyl alcohol are consistent with the current work, whereas the rearomatization energies are somewhat more exergonic. Rearomatization energies of other combinations are more exergonic than those in which diferuloylputrescine is the lignin monomer, but the former can result in the formation of six-membered ring benzodioxanes rather than the acyclic 8-O-4' and β'-O-4 linkages in the current work.

The energies of reaction for quinone methide formation through the 8-5'/5'-β linkage among the hydroxystilbene glucosides vary from −14.6 to −26.7 kcal mol^{-1}, such that those involving diferuloylputrescine are intermediate. Rearomatization energies are similar in the −30 to −40 kcal mol^{-1} range.

As mentioned in the Results section, the *cis* configuration of the phenylcoumaran ring resulting from 8 to 5′ homo-coupling of diferuloylputrescine is found to be the more stable stereoisomer. In contrast, for the 8-5′ and β-5′ cross-coupled dimers the *trans* stereoisomer is more stable. Experimental results, however, have routinely found that phenylcoumaran rings in lignin are in the *trans* configuration (Li et al., 1997;

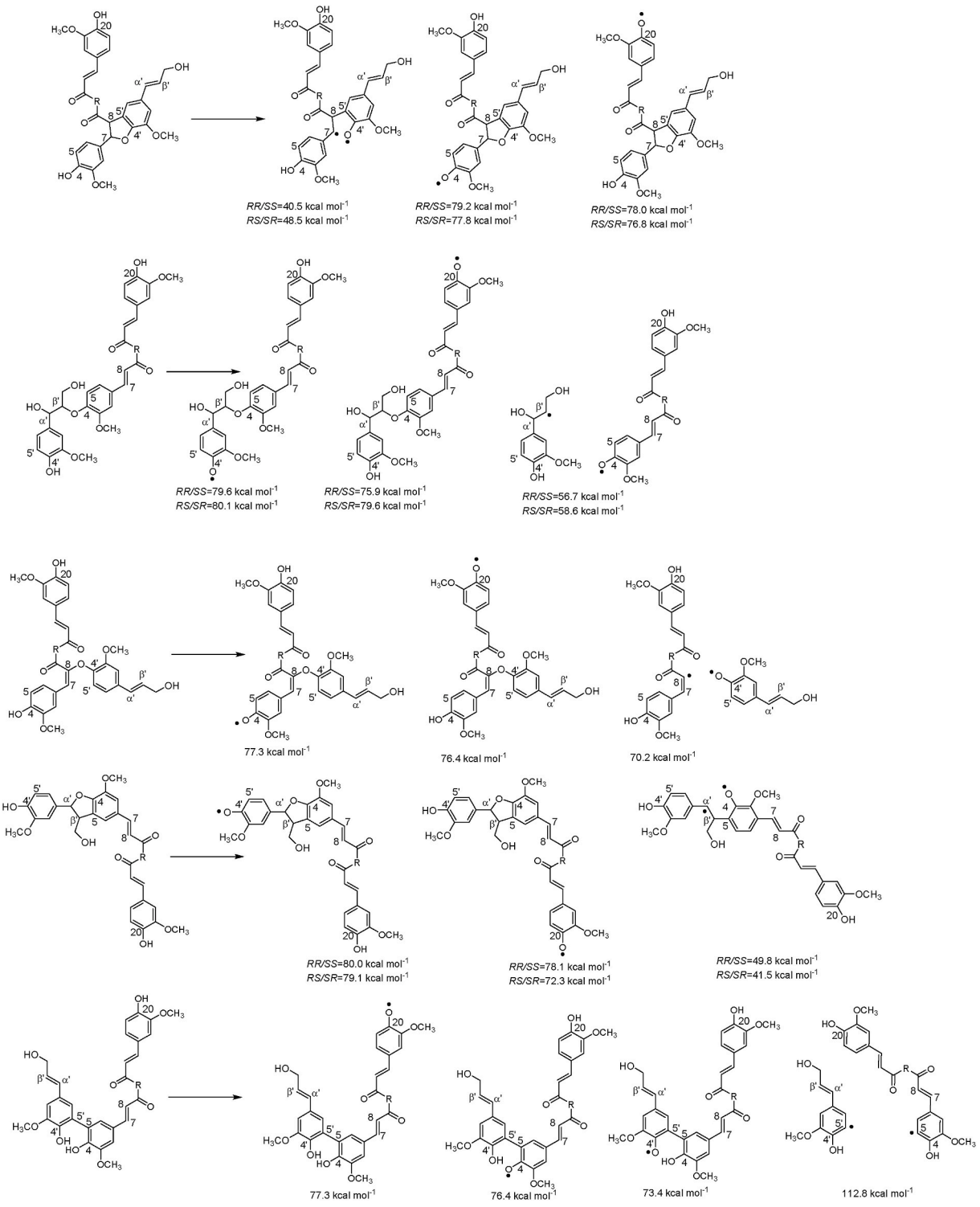

Fig. 7. Gibbs free energy of reaction for dehydrogenation and bond dissociation of cross-coupled diferuloylputrescine-coniferyl alcohol dimers.

Ralph et al., 2009).

Although it might be fortuitous if the calculated results were in agreement with experiment, it must be borne in mind that the formation of dimers is a multi-step process involving radical formation, coupling, and rearomatization. Based on a review of quinone methides in lignification, there are still questions about which of these is the rate-determining step and if dimer formation is under thermodynamic or kinetic control (Ralph et al., 2009). Furthermore, the preponderance of *trans* stereochemistry in lignin notwithstanding, direct evidence for the configuration of dimers involving diferuloylputrescine is not available. If for the sake of argument, however, it is assumed that the rearomatization is the rate-determining step, results for which the *cis* configuration is more stable would provide circumstantial evidence for kinetic control.

With respect to interunit linkages, previous experimental work on the cross-coupling of coniferyl alcohol with ethyl ferulate (Zhang et al., 2009) has reported on the occurrence of β-O-4′, β-5′ and 8-5′ combinations, but 8-O-4′ and 5-5′ were not detected. For the sake of

completeness, the current work includes the latter documenting their thermodynamic feasibility to show that they could occur with coniferyl alcohol-diferuloylputrescine cross-couples while awaiting experimental results.

The energies of reactions that have been reported throughout the current paper have exclusively involved neutral products and reactants. Furthermore, all results are from gas-phase calculations. The latter is justified by the former as the energetics of neutral species are less sensitive to solvation than for ionic reactions. That notwithstanding, it is acknowledged that solvation could have an effect on conformation and, in turn, the energetics. It was found, however, that with solvation the diferuloylputrescine monomer and its radical retained the folded and highly parallel conformation observed in the gas phase. Optimally, any differences between computational and experimental results, such as seen in the configuration of 8–5′ homo-coupled diferuloylputrescine, could be obviated by the use of even higher-level calculations with solvation. Computational studies, such as the current one, are always a compromise between the ideal calculations and the practical issues of computer time and memory requirements, especially for structures of the size examined in this work. It is anticipated that as technology and computational methods advance such work can be revisited and the results reassessed, ideally with additional experimental data.

4. Conclusions

As discussed in the Introduction, additional evidence of cross-coupling, and the nature thereof, between diferuloylputrescine and lignin awaits further experimental confirmation. This notwithstanding, the current work demonstrates the thermodynamic feasibility of such reactions, finding values for radical coupling and rearomatization that are similar to those found for other non-conventional lignin monomers and the canonical monolignols. Furthermore, the energies of the dehydrogenation reactions, essential for incorporation into the lignin polymer are generally consistent with previously reported values for both monolignols and alternative lignin monomers. These results show that there is no thermodynamic impediment to the formation of bonds between diferuloylputrescine and monolignols and that, once formed, such coupling products could feasibly undergo the subsequent dehydrogenation step needed for true polymerization. With respect to conformation, particularly for the highly folded diferuloylputrescine, it must be borne in mind that the current calculations have been carried out on isolated molecules in which pi-stacking and other non-bonded interactions may be dominant. It is acknowledged that within the complex cell wall environment, interactions could occur with other, particularly aromatic, moieties potentially altering the conformation. At the present time, however, information describing the composition and orientation of the constituents of the cell wall at the atomistic level is not available. Future advances in detailed cell wall structure are anticipated that will allow for such interactions to be taken into account in ongoing computational efforts.

5. Experimental

The reactions of diferuloylputrescine examined in the current study are as shown in Figs. 3 and 4. The initial step (Fig. 1) is concerned with the oxidation of diferuloylputrescine, whereas quinone methide formation through radical coupling and rearomatization of the homo-coupled and diferuloylputrescine cross-coupled with coniferyl alcohol dimers are shown in Figs. 3 and 4, respectively. As enantiomers have identical physical properties, other than the rotation of plane polarized light, calculations were performed on one set of enantiomers, in structures with chiral carbons.

Due to the number of rotatable bonds, these structures can exhibit considerable flexibility, such that a conformational search is essential for identifying stable conformations. This was accomplished using a 5000-step Monte Carlo search and optimization with the Merck force field (MMFF) after which conformations within 50 kJ mol^{-1} of the minimum were optimized with the PM6 semi-empirical method as implemented in Spartan'18 (2018). The 20 low-energy conformations were further refined using the M06–2X density functional method with the 6-31+G(d) basis set and the GD3 empirical dispersion correction. The lowest energy conformation from this step was finally optimized with M06–2X/6–311++G(d,p), the GD3 empirical dispersion and a frequency calculation at 298.15 K to verify the identification of a local minimum and for thermal corrections to the electronic energy. The density functional theory calculations were all performed with Gaussian 16 (Frisch et al., 2019), using default optimization criteria and the ultrafine integration grid. The values reported throughout are Gibbs free energy at 298.15 K. For the coupling reactions shown in Figs. 3 and 4, the radical reactants were modeled as neutral doublets and all other closed-shell products as neutral singlets. The optimized geometries of the dimers were used as the starting structures for the dehydrogenation reactions and bond dissociation energy calculations. Appropriate hydrogens and bonds were removed followed by geometry optimization of the open-shell products, such that the nearest local minimum is identified. For ring-opening reactions the interatomic distance was started at 2.5 Å to prevent reformation of the salient bond. The dehydrogenation products and ring opened products, shown in Figs. 6 and 7, were modeled as neutral doublets and neutral triplets, respectively. Solvation effects of water on the geometry of diferuloylputrescine were evaluated at the M062X/6–311++G(d,p) level of theory using the SMD method.

Declaration of competing interest

The authors declare that they have no known competing financial interests or personal relationships that could have appeared to influence the work reported in this paper.

Acknowledgments

This work used the Extreme Science and Engineering Discovery Environment (XSEDE), which is supported by National Science Foundation grant number ACI-1548562. Specifically, it used the Bridges system at the Pittsburgh Supercomputing Center (PSC), Comet at the San Diego Supercomputer Center and Stampede2 at the Texas Advanced Computing Center (TACC), both via MCB-090159. This work was also made possible in part by a grant of high performance computing resources and technical support from the Alabama Supercomputer Authority. JR and HK were funded by the DOE Great Lakes Bioenergy Research Center (DOE Office of Science BER DE-SC0018409). JRe and JCdR were funded by the Spanish Projects PID2020-118968RB-I00 and AGL2017-83036-R (financed by Agencia Estatal de Investigación, AEI and Fondo Europeo de Desarrollo Regional, FEDER), and by the Junta de Andalucía (project P20-00017). This research was supported in part by the U.S. Department of Agriculture, U.S. Forest Service.

References

Bauer, J.L., Harbaum-Piayda, B., Schwarz, K., 2012. Phenolic compounds from hydrolyzed and extracted fiber-rich by-products. LWT - Food Sci. Technol. (Lebensmittel-Wissenschaft -Technol.) 47, 246–254. https://doi.org/10.1016/j.lwt.2012.01.012.

Bauer, J.L., Harbaum-Piayda, B., Stöckmann, H., Schwarz, K., 2013. Antioxidant activities of corn fiber and wheat bran and derived extracts. LWT - Food Sci. Technol. (Lebensmittel-Wissenschaft -Technol.) 50, 132–138. https://doi.org/10.1016/j.lwt.2012.06.012.

Berstis, L., Elder, T., Crowley, M., Beckham, G.T., 2016. Radical nature of C-lignin. ACS Sustain. Chem. Eng. 4, 5327–5335. https://doi.org/10.1021/acssuschemeng.6b00520.

Berstis, L., Elder, T., Dixon, R., Crowley, M., Beckham, G., 2020. Coupling of flavonoid initiation sites with monolignols studied by density functional theory. ACS Sustain. Chem. Eng. 9, 1518–1528. https://doi.org/10.1021/acssuschemeng.0c04240.

Chen, F., Tobimatsu, Y., Havkin-Frenkel, D., Dixon, R.A., Ralph, J., 2012. A polymer of caffeyl alcohol in plant seeds. Proc. Natl. Acad. Sci. U. S. A 109, 1772–1777. https://doi.org/10.1073/pnas.1120992109.

del Río, J.C., Marques, G., Rencoret, J., Martínez, Á.T., Gutiérrez, A., 2007. Occurrence of naturally acetylated lignin units. J. Agric. Food Chem. 55, 5461–5468. https://doi.org/10.1021/jf0705264.

del Río, J.C., Rencoret, J., Gutierrez, A., Elder, T., Kim, H., Ralph, J., 2020. Lignin monomers from beyond the canonical monolignol biosynthetic pathway – another brick in the wall. ACS Sustain. Chem. Eng. 8, 4997–5012. https://doi.org/10.1021/acssuschemeng.0c01109.

del Río, J.C., Rencoret, J., Gutiérrez, A., Kim, H., Ralph, J., 2018. Structural characterization of lignin from maize (*Zea mays* L.) fibers: evidence for diferuloylputrescine incorporated into the lignin polymer in maize kernels. J. Agric. Food Chem. 66, 4402–4413. https://doi.org/10.1021/acs.jafc.8b00880.

del Río, J.C., Rencoret, J., Gutiérrez, A., Kim, H., Ralph, J., 2017. Hydroxystilbenes are monomers in palm fruit endocarp lignins. Plant Physiol. 174, 2072–2082. https://doi.org/10.1104/pp.17.00362.

del Río, J.C., Rencoret, J., Gutiérrez, A., Lan, W., Kim, H., Ralph, J., 2021. Lignin monomers derived from the flavonoid and hydroxystilbene biosynthetic pathways. In: Reed, J.D., de Freitas, V.A.P., Quideau, S. (Eds.), Recent Advances in Polyphenol Research, ume 7. Wiley Online Books. John Wiley & Sons Ltd, pp. 177–206. https://doi.org/10.1002/9781119545958.ch7.

del Río, J.C., Rencoret, J., Marques, G., Gutiérrez, A., Ibarra, D., Santos, J.I., Jiménez-Barbero, J., Zhang, L., Martínez, Á.T., 2008. Highly acylated (acetylated and/or *p*-coumaroylated) native lignins from diverse herbaceous plants. J. Agric. Food Chem. 56, 9525–9534. https://doi.org/10.1021/jf800806h.

del Río, J.C., Rencoret, J., Prinsen, P., Martínez, A.T., Ralph, J., Gutiérrez, A., Martínez, Á.T., Ralph, J., Gutiérrez, A., 2012. Structural characterization of wheat straw lignin as revealed by analytical pyrolysis, 2D-NMR, and reductive cleavage methods. J. Agric. Food Chem. 60, 5922–5935. https://doi.org/10.1021/jf301002n.

Elder, T., Berstis, L., Beckham, G.T., Crowley, M.F., 2016. Coupling and reactions of 5-hydroxyconiferyl alcohol in lignin formation. J. Agric. Food Chem. 64, 4742–4750. https://doi.org/10.1021/acs.jafc.6b02234.

Elder, T., Carlos del Río, J., Ralph, J., Rencoret, J., Kim, H., Beckham, G.T., 2019. Radical coupling reactions of piceatannol and monolignols: a density functional theory study. Phytochemistry 164, 12–23. https://doi.org/10.1016/j.phytochem.2019.04.003.

Elder, T., del Río, J.C., Ralph, J., Rencoret, J., Kim, H., Beckham, G.T., Crowley, M.F., 2020. Coupling and reactions of lignols and new lignin monomers: a density functional theory study. ACS Sustain. Chem. Eng. 8, 11033–11045. https://doi.org/10.1021/acssuschemeng.0c02880.

Elder, T., Rencoret, J., del Río, J.C., Kim, H., Ralph, J., 2021. Radical coupling reactions of hydroxystilbene glucosides and coniferyl alcohol: a density functional theory study. Front. Plant Sci. 12, 1–13. https://doi.org/10.3389/fpls.2021.642848.

Frisch, M.J., Trucks, G.W., Schlegel, H.B., Scuseria, G.E., Robb, M.A., Cheeseman, J.R., Scalmani, G., Barone, V., Petersson, G.A., Nakatsuji, H., Li, X., Caricato, M., Marenich, A.V., Bloino, J., Janesko, B.G., Gomperts, R., Mennucci, B., Hratchian, H. P., Ortiz, J.V., Izmaylov, A.F., Sonnenberg, J.L., Williams Ding, F., Lipparini, F., Egidi, F., Goings, J., Peng, B., Petrone, A., Henderson, T., Ranasinghe, D., Zakrzewski, V.G., Gao, J., Rega, N., Zheng, G., Liang, W., Hada, M., Ehara, M., Toyota, K., Fukuda, R., Hasegawa, J., Ishida, M., Nakajima, T., Honda, Y., Kitao, O., Nakai, H., Vreven, T., Throssell, K., Montgomery Jr., J.A., Peralta, J.E., Ogliaro, F., Bearpark, M.J., Heyd, J.J., Brothers, E.N., Kudin, K.N., Staroverov, V.N., Keith, T.A., Kobayashi, R., Normand, J., Raghavachari, K., Rendell, A.P., Burant, J.C., Iyengar, S. S., Tomasi, J., Cossi, M., Millam, J.M., Klene, M., Adamo, C., Cammi, R., Ochterski, J. W., Martin, R.L., Morokuma, K., Farkas, O., Foresman, J.B., Fox, D.J., 2019. Gaussian 16, Revision C.01. Gaussian, Inc., Wallingford CT, 2019.

Karlen, S.D., Smith, R.A., Kim, H., Padmakshan, D., Bartuce, A., Mobley, J.K., Free, H.C. A., Smith, B.G., Harris, P.J., Ralph, J., 2017. Highly decorated lignins in leaf tissues of the canary island date palm *Phoenix canariensis*. Plant Physiol. 175, 1058–1067. https://doi.org/10.1104/pp.17.01172.

Karlen, S.D., Zhang, C., Peck, M.L., Smith, R.A., Padmakshan, D., Helmich, K.E., Free, H. C.A., Lee, S., Smith, B.G., Lu, F., Sedbrook, J.C., Sibout, R., Grabber, J.H., Runge, T. M., Mysore, K.S., Harris, P.J., Bartley, L.E., Ralph, J., 2016. Monolignol ferulate conjugates are naturally incorporated into plant lignins. Sci. Adv. 2 https://doi.org/10.1126/sciadv.1600393.

Kim, E.O., Min, K.J., Kwon, T.K., Um, B.H., Moreau, R.A., Choi, S.W., 2012. Anti-inflammatory activity of hydroxycinnamic acid derivatives isolated from corn bran in lipopolysaccharide-stimulated Raw 264.7 macrophages. Food Chem. Toxicol. 50, 1309–1316. https://doi.org/10.1016/j.fct.2012.02.011.

Kim, H., Li, Q., Karlen, S.D., Smith, R.A., Shi, R., Liu, J., Yang, C., Tunlaya-Anukit, S., Wang, J.P., Chang, H.-M.M., Sederoff, R.R., Ralph, J., Chiang, V.L., 2020. Monolignol benzoates incorporate into the lignin of transgenic Populus trichocarpa depleted in C3H and C4H. ACS Sustain. Chem. Eng. 8, 3644–3654. https://doi.org/10.1021/acssuschemeng.9b06389.

Kim, M.J., Kim, S.M., Im, K.R., Yoon, K.S., 2010. Effect of hydroxycinnamic acid derivatives from corn bran on melanogenic protein expression. J. Appl. Biol. Chem. 53, 422–426. https://doi.org/10.3839/jksabc.2010.065.

Kim, S., Chmely, S.C., Nimlos, M.R., Bomble, Y.J., Foust, T.D., Paton, R.S., Beckham, G. T., 2011. Computational study of bond dissociation enthalpies for a large range of native and modified Lignins. J. Phys. Chem. Lett. 2, 2846–2852. https://doi.org/10.1021/jz201182w.

Kudanga, T., Nugroho Prasetyo, E., Sipilä, J., Eberl, A., Nyanhongo, G.S., Guebitz, G.M., 2009. Coupling of aromatic amines onto syringylglycerol β-guaiacylether using Bacillus SF spore laccase: a model for functionalization of lignin-based materials. J. Mol. Catal. B Enzym. 61, 143–149. https://doi.org/10.1016/j.molcatb.2009.06.003.

Lan, W., Lu, F., Regner, M., Zhu, Y., Rencoret, J., Ralph, S.A., Zakai, U.I., Morreel, K., Boerjan, W., Ralph, J., 2015. Tricin, a flavonoid monomer in monocot lignification. Plant Physiol. 167, 1284–1295. https://doi.org/10.1104/pp.114.253757.

Lan, W., Morreel, K., Lu, F., Rencoret, J., del Río, J.C., Voorend, W., Vermerris, W., Boerjan, W.A., Ralph, J., 2016a. Maize tricin-oligolignol metabolites and their implications for monocot lignification. Plant Physiol. 171 https://doi.org/10.1104/pp.16.02012, 201602012.

Lan, W., Rencoret, J., Lu, F., Karlen, S.D., Smith, B.G., Harris, P.J., del Río, J.C., Ralph, J., 2016b. Tricin-lignins: occurrence and quantitation of tricin in relation to phylogeny. Plant J. 88, 1046–1057. https://doi.org/10.1111/tpj.13315.

Li, S., Iliefski, T., Lundquist, K., Wallis, A.F.A., 1997. Reassignment of relative stereochemistry at C-7 and C-8 in arylcoumaran neolignans. Phytochemistry 46, 929–934. https://doi.org/10.1016/S0031-9422(97)00360-9.

Lu, F., Karlen, S.D., Regner, M., Kim, H., Ralph, S.A., Sun, R.C., Kuroda, K. ichi, Augustin, M.A., Mawson, R., Sabarez, H., Singh, T., Jimenez-Monteon, G., Zakaria, S., Hill, S., Harris, P.J., Boerjan, W., Wilkerson, C.G., Mansfield, S.D., Ralph, J., 2015. Naturally *p*-hydroxybenzoylated lignins in palms. Bioenergy Res. 8, 934–952. https://doi.org/10.1007/s12155-015-9583-4.

Mahmoud, A.B., Danton, O., Kaiser, M., Han, S., Moreno, A., Abd Algaffar, S., Khalid, S., Oh, W.K., Hamburger, M., Mäser, P., 2020. Lignans, amides, and saponins from *Haplophyllum tuberculatum* and their antiprotozoal activity. Molecules 25, 2825. https://doi.org/10.3390/molecules25122825.

Mellon, J.E., Moreau, R.A., 2004. Inhibition of aflatoxin biosynthesis in *Aspergillus flavus* by diferuloylputrescine and *p*-coumaroylferuloylputrescine. J. Agric. Food Chem. 52, 6660–6663. https://doi.org/10.1021/jf040226b.

Moreau, R.A., Hicks, K.B., 2005. The composition of corn oil obtained by the alcohol extraction of ground corn. JAOCS, J. Am. Oil Chem. Soc. 82, 809–815. https://doi.org/10.1007/s11746-005-1148-4.

Moreau, R.A., Nuñez, A., Singh, V., 2001. Diferuloylputrescine and p-coumaroyl-feruloylputrescine, abundant polyamine conjugates in lipid extracts of maize kernels. Lipids 36, 839–844. https://doi.org/10.1007/s11745-001-0793-6.

Negrel, J., Pollet, B., Lapierre, C., 1996. Ether-linked ferulic acid amides in natural and wound periderms of potato tuber. Phytochemistry 43, 1195–1199. https://doi.org/10.1016/S0031-9422(96)00500-6.

Niwa, T., Doi, U., Osawa, T., 2003. Inhibitory activity of corn-derived bisamide compounds against α-glucosidase. J. Agric. Food Chem. 51, 90–94. https://doi.org/10.1021/jf020758x.

Ralph, J., Hatfield, R.D., Piquemal, J., Yahiaoui, N., Pean, M., Lapierre, C., Boudet, A.M., 1998. NMR characterization of altered lignins extracted from tobacco plants down-regulated for lignification enzymes cinnamyl-alcohol dehydrogenase and cinnamoyl-CoA reductase. Proc. Natl. Acad. Sci. U. S. A 95, 12803–12808. https://doi.org/10.1073/pnas.95.22.12803.

Ralph, J., Kim, H., Lu, F., Smith, R.A., Karlen, S.D., Nuoendagula Eugene, A., Liu, S., Sener, C., Ando, D., Chen, M., Li, Y., Landucci, L.L., Ralph, S.A., Timokhin, V.I., Rencoret, J., del Río, J.C., 2021. Lignins and lignification: new developments and emerging concepts. In: Quideau, S. (Ed.), Recent Advances in Polyphenol Research, Volume 8. John Wiley & Sons Ltd (in press).

Ralph, J., Lapierre, C., Boerjan, W., 2019. Lignin structure and its engineering. Curr. Opin. Biotechnol. 56, 240–249. https://doi.org/10.1016/j.copbio.2019.02.019.

Ralph, J., Lapierre, C., Lu, F., Marita, J.M., Pilate, G., Van Doorsselaere, J., Boeŕjan, W., Jouanin, L., 2001. NMR evidence for benzodioxane structures resulting from incorporation of 5-hydroxyconiferyl alcohol into lignins of O-methyltransferase-deficient poplars. J. Agric. Food Chem. 49, 86–91. https://doi.org/10.1021/jf001042+.

Ralph, J., MacKay, J.J., Hatfield, R.D., O'Malley, D.M., Whetten, R.W., Sederoff, R.R., 1997. Abnormal lignin in a loblolly pine mutant. Science (80- 277, 235–239. https://doi.org/10.1126/science.277.5323.235.

Ralph, J., Schatz, P.F., Lu, F., Kim, H., Akiyama, T., Nelsen, S.F., 2009. Quinone methides in lignification. Quinone Methides 385–420. https://doi.org/10.1002/9780470452882.ch12.

Rencoret, J., Kim, H., Evaristo, A.B., Gutiérrez, A., Ralph, J., del Río, J.C., 2018. Variability in lignin composition and structure in cell walls of different parts of macaúba (*Acrocomia aculeata*) palm fruit. J. Agric. Food Chem. 66, 138–153. https://doi.org/10.1021/acs.jafc.7b04638.

Rencoret, J., Neiva, D., Marques, G., Gutiérrez, A., Kim, H., Gominho, J., Pereira, H., Ralph, J., Del Río, J.C., 2019. Hydroxystilbene glucosides are incorporated into Norway spruce bark lignin. Plant Physiol. 180, 1310–1321. https://doi.org/10.1104/pp.19.00344.

Sangha, A.K., Davison, B.H., Standaert, R.F., Davis, M.F., Smith, J.C., Parks, J.M., 2014. Chemical factors that control lignin polymerization. J. Phys. Chem. B 118, 164–170. https://doi.org/10.1021/jp411998t.

Sangha, A.K., Parks, J.M., Standaert, R.F., Ziebell, A., Davis, M., Smith, J.C., 2012. Radical coupling reactions in lignin synthesis: a density functional theory study. J. Phys. Chem. B 116, 4760–4768. https://doi.org/10.1021/jp2122449.

Sinnokrot, M.O., Sherrill, C.D., 2004. Highly accurate coupled cluster potential energy curves for the benzene dimer: sandwich, T-shaped, and parallel-displaced configurations. J. Phys. Chem. 108, 10200–10207. https://doi.org/10.1021/jp0469517.

Spartan'18, 2018. Spartan'18 Wavefunction, Inc., Irvine, CA.

Vanholme, R., De Meester, B., Ralph, J., Boerjan, W., 2019. Lignin biosynthesis and its integration into metabolism. Curr. Opin. Biotechnol. 56, 230–239. https://doi.org/10.1016/j.copbio.2019.02.018.

Yoshimura, M., Ochi, K., Sekiya, H., Tamai, E., Maki, J., Tada, A., Sugimoto, N., Akiyama, H., Amakura, Y., 2017. Identification of characteristic phenolic

constituents in mousouchiku extract used as food additives. Chem. Pharm. Bull. 65, 878–882. https://doi.org/10.1248/cpb.c17-00401.

Zhang, A., Lu, F., Sun, R., Ralph, J., 2009. Ferulate-coniferyl alcohol cross-coupled products formed by radical coupling reactions. Planta 229, 1099–1108. https://doi.org/10.1007/s00425-009-0894-6.

Zhao, Y., Truhlar, D.G., 2008. The M06 suite of density functionals for main group thermochemistry, thermochemical kinetics, noncovalent interactions, excited states, and transition elements: two new functionals and systematic testing of four M06-class functionals and 12 other function. Theor. Chem. Acc. 120, 215–241. https://doi.org/10.1007/s00214-007-0310-x.